

# Prediction of Five Points Bending Spring-back of TC4 Titanium Alloy Plate Based on Variable Elastic Modulus

Qu Cong<sup>1</sup>, Wang Dongjie<sup>2</sup>

<sup>1</sup> College of mechanical engineering, Taiyuan University of science and technology, Tai'yuan 030000, China; <sup>2</sup> School of mechanical and electrical engineering, China University of Mining and Technology (Beijing), Bei'jing 100083, China

**Abstract:** TC4 titanium alloy material will generate significant spring back during the bending process, and its elastic modulus has a significant impact on spring back. However, previous studies have not considered the change in elastic modulus during the plastic strain change process of the material. This study focuses on TC4 titanium alloy and conducts uniaxial tensile and cyclic loading unloading experiments to determine the anisotropy parameters and the variation of material elastic modulus with plastic strain. On this basis, a mathematical model for the variable elastic modulus of TC4 titanium alloy was established. Based on three different constitutive models, namely YLD2000-2D yield criterion and variable elastic modulus, YLD2000-2D anisotropy, and Mises isotropy, numerical simulations were conducted on the five point bending process of TC4 titanium alloy plates at room temperature. In order to verify the numerical simulation results, a five point bending experiment was conducted on TC4 sheets at room temperature. The results showed that the anisotropic constitutive model and the mathematical model of variable elastic modulus significantly improved the prediction accuracy of TC4 titanium alloy bending spring back, the highest prediction accuracy increased by 31.18%.

**Key words:** Titanium alloy; Bending forming; Variable elastic modulus; Spring back prediction

TC4 titanium alloy has been successfully applied in aviation, medical, automotive manufacturing, marine and other fields due to its excellent material properties such as low density, high specific strength, and good fatigue resistance<sup>[1-3]</sup>. However, due to its high yield strength and low elastic modulus, it is difficult to control the spring back of TC4 titanium alloy during bending forming. Therefore, predicting the spring back during bending is of great significance for product quality. Jun Z et al.<sup>[4]</sup> established a mechanical model for tensile bending of profiles based on classical elastic-plastic theory and strain superposition characteristics, and verified the theoretical analysis with U-shaped and rectangular cross-sections. Li Hao et al.<sup>[5]</sup> established a theoretical model considering both the effects of the space-time deformation history and the strain rate to predict the spring-back behaviors. In the proposed model, a novel shape equation is established to describe the space-time deformation history of sheet. A. Maati<sup>[6]</sup> et al. demonstrated the influence of

constitutive model on the prediction of SB degree in tensile bending test through numerical simulation. U. M. Mert<sup>[7]</sup> and other scholars have studied the deformation behavior of TC4 titanium alloy at high temperature and believe that the extended Ludwik model is more suitable for modeling the mechanical behavior within the forming temperature range.

Finite element simulation is an effective method for predicting material bending spring back. In recent years, many scholars have flexibly applied finite element simulation to the forming process of materials and achieved good results in solving real problems. Esat et al.<sup>[8]</sup> used finite software to conduct reverse simulation analysis on the bending spring back of different aluminum alloy materials with different thicknesses. They provided the spring back amount, total equivalent plastic strain, and equivalent Mises stress, and observed that the spring back increased with the increase of yield strength. Wang Yan et al.<sup>[9]</sup> studied the effect of spring back on the wall thickness reduction and section distortion of TA18 high-strength titanium tubes

Received date:

Foundation item: NSFC(52004169)

Corresponding author: Wang Dongjie, School of mechanical and electrical engineering, China University of Mining and Technology (Beijing), Bei'jing 100083, P. R. China, Tel: 18705217011, E-mail: wdj@student.cumt.edu.cn

Copyright ©, Northwest Institute for Nonferrous Metal Research. Published by Science Press. All rights reserved.

using ABAQUS finite element explicit/implicit methods. The results showed that the wall thickness reduction rate after unloading and spring back of high-strength titanium tubes was less than 10%, and the section distortion rate was greater than 35%, even exceeding 60%. Myoung Yu Lee et al.<sup>[10]</sup> provided a plane stress formula for shell components and used finite element software to simulate the spring back of sheet metal. They examined the effects of deformation plasticity, volume strain, and cooling rate on spring back. Among the influencing factors in finite element simulation, the constitutive model is particularly important for the simulation results. When studying the anisotropy of plastic properties of steel plates, scholars such as Zhu J et al.<sup>[11]</sup> take into account the correlation and non correlation flow rules of the Hill48 yield criterion, and provide suggestions for the use of flow rules in simulating high-strength steel using the Hill48 yield criterion. Yang Xiao Ming et al.<sup>[12]</sup> studied the spring back of TC4 titanium alloy under hot stamping conditions through experiments and numerical analysis. Scholars such as J W Yoon et al.<sup>[13]</sup> proposed that the YLD2000-2D yield criterion is applicable to the plane stress state. This yield criterion uses two linear transformations to introduce the anisotropic parameters of the material into the function and applies it to numerical simulation. Barlat et al.<sup>[14]</sup> proposed the YLD2000-2D yield criterion and applied it to finite element analysis of the forming process of aluminum alloy sheets. Naofal et al.<sup>[15]</sup> studied the prediction of spring back during sheet metal roll bending process, indicating that the change in elastic modulus plays an important role in bending forming. Chaboche<sup>[16]</sup> improved the nonlinear dynamic hardening model (A-F) to demonstrate the phenomenon of material hardening.

Elastic modulus is one of the important mechanical performance parameters in the process of material bending and forming, and it is also a key influencing factor for the spring back of material deformation after external force unloading. Badr et al.<sup>[17]</sup> studied room temperature roll bending of titanium alloys and proposed an anisotropic elastic-plastic constitutive material model. Dongwei Ao et al.<sup>[18]</sup> studied the effect of electric pulse frequency and peak current density on the spring back behavior of Ti-6Al-4V titanium alloy. The results show that the spring back angle and V-shaped bending load decrease with the increase of frequency and peak current density. The results showed that it is closer to the experiment. Chai<sup>[19]</sup> used the extended regression mapping algorithm to consider the reduction of elastic modulus in the plastic constitutive model and simulated the forming and spring back of DP600 steel U-shaped parts. The results showed that the accuracy of spring back simulation was significantly improved when the elastic modulus was reduced as described in the model. Hai<sup>[20]</sup> proposed an empirical expression for the relationship between elastic modulus and plastic strain, and applied it to LS-DYNA software for spring back simulation of U-shaped steel. The results showed that the accuracy of spring back simulation considering changes in elastic modulus was higher. Yoshida et al.<sup>[21]</sup> found that the

elastic modulus decreases with increasing pre strain when studying high-strength steel. Yuan Chen et al.<sup>[22]</sup> Developed a physical based integrated constitutive model to describe stress relaxation. Based on the principle of increasing temperature to enhance stress relaxation, it is found that increasing the forming speed is an effective way to reduce the spring back of titanium alloy in hot stamping. Cong Liu et al.<sup>[23]</sup> introduced the influence of the bending and spring back process of titanium tubes with different bending radius and bending angle on the spring back rate after unloading, and analyzed the distribution of titanium tubes and the changes of stress and strain. The study showed that the elastic modulus rapidly decreases with the increase of plastic pre strain and eventually tends to flatten.

This article investigates the anisotropy and elastic modulus variation of TC4 titanium alloy tensile specimens through uniaxial tensile and cyclic loading unloading experiments, and establishes a mathematical model for variable elastic modulus. Based on three different constitutive models: YLD2000-2D yield criterion and variable elastic modulus, YLD2000-2D anisotropy, and Mises isotropy, numerical simulations of spring back in five points bending of sheet metal were conducted using ABAQUS simulation software. Finally, a five point bending experiment was conducted on TC4 titanium alloy plates at room temperature, and the experimental and simulation results were compared and analyzed.

## 1 Material selection

Titanium is an allotrope with two different crystal structures. It is called  $\alpha$ -Ti below 882°C and  $\beta$ -Ti above 882°C.  $\alpha$ -Ti is an ideal densely packed hexagonal (HCP) structure, and  $\beta$ -Ti has a body centered cubic crystal structure. TC4 titanium alloy, as an equiaxed microstructure alloy with  $\alpha+\beta$  phases, has good comprehensive properties and can be subjected to thermal stress processing well. It can also be strengthened by quenching and aging treatment. Its main constituent elements and content are shown in Table 1.

**Table 1 Material chemical composition**

Element	Proportion/%
Ti	Rest
Fe	0.3
C	0.08
N	0.05
H	0.015
O	0.2
Al	6.5
V	4.5

## 2 Experiment, constitutive establishment, and numerical simulation

### 2.1 Uniaxial tensile and cyclic loading unloading

## experiments

To obtain the anisotropy parameters of TC4 titanium alloy, tensile experiments were conducted in three directions: RD (rolling direction), DD (diagonal direction), and TD (transverse direction). The experiment was conducted on the instron-5969 universal material testing machine, with a tensile rate of 0.01mm/min, and deformation was measured using a contact extensometer. The size of the tensile specimens used in the experiment are shown in Figures 1.

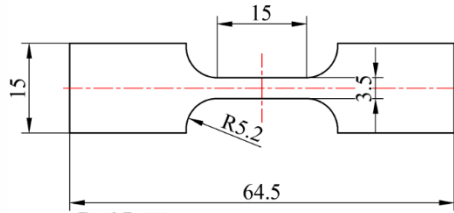


Fig.1 The size of the tensile specimen

The variation law of elastic modulus in different directions was studied through cyclic loading unloading experiments, which were under the same experimental conditions as the tensile experiment. Set different pre strains to test the material properties in the RD, DD, and TD directions through a cyclic testing process of loading unloading. The pre strain is sequentially set as 0.8%, 1.0%, 1.5%, 2%, 2.5%, 3.3%, 4.1%, 5.1%, 6.1%, 7.1%, 8.1%, and 9.1%.

## 2.2 Analysis of experimental results

The stress-strain curves of TC4 titanium alloy tensile specimens in the RD, DD, and TD directions were obtained through the uniaxial tensile test in section 2.1, as shown in Figure 2.

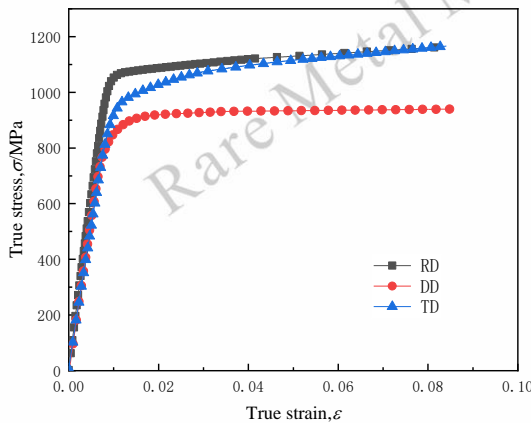


Fig.2 TC4 titanium alloy stress-strain curves

The material parameters of TC4 titanium alloy in three directions: modulus of elasticity ( $E_0$ ), 0.2% offset yield strength ( $\sigma_s$ ), ultimate tensile strength ( $\sigma_U$ ), total elongation, and plastic-to-strain ratio ( $r$ ) were measured in tensile experiments, as shown in Table 2.

Plastic strain ratio  $r$ :

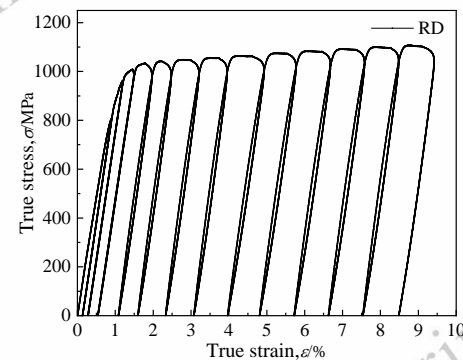
$$r = \frac{\varepsilon_w}{\varepsilon_t} = \frac{\ln \frac{\omega}{\omega_0}}{\ln \frac{t}{t_0}} \quad (1)$$

Where:  $\varepsilon_w, \varepsilon_t$ —strain in width direction, thickness direction;  
 $\omega_0, \omega$ —initial width, final width;  
 $t_0, t$ —Initial thickness, final thickness of the specimen

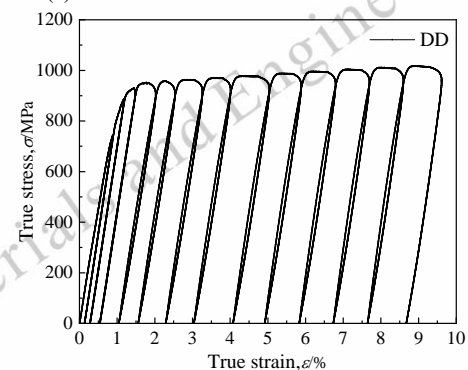
Table 2 Material parameters of TC4 titanium alloy

obtained from uniaxial tensile test			
Direction	RD	DD	TD
Elastic modulus $E_0$ /GPa	120	113	110
0.2% offset yield strength $\sigma_s$ /MPa	1042	851	936
ultimate tensile strength $\sigma_U$ /MPa	1159	943	1168
total elongation /%	12.3	13.6	11.5
plastic strain ratio $r$	2.52	3.73	3.11

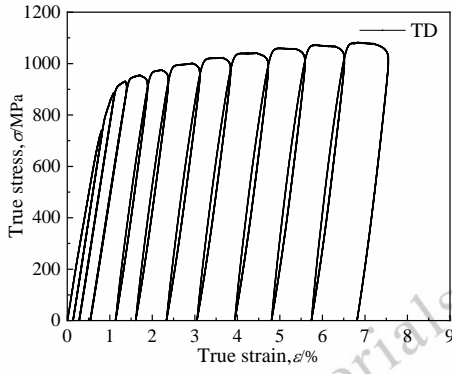
The stress-strain curves in the three directions of RD, DD and TD were measured by cyclic loading-unloading experiments, as shown in Fig.3.



(a) Stress-strain curves in the RD direction



(b) Stress-strain curves in the DD direction



(c) Stress-strain curves in the TD direction

Fig.3 Stress-strain curve of loading and unloading experiment

### 2.3 Definition of variable elastic modulus

There are three ways of calculating the modulus of elasticity: loaded modulus, unloaded modulus, and chordal modulus. Naofal et al. verified that the chordal modulus has higher accuracy for predicting the spring back as compared to the loaded and unloaded moduli (Ref. 15). The chord modulus is calculated as follows:

$$E_u = \frac{(\sigma_1 - \sigma_0)}{(\varepsilon_1 - \varepsilon_0)} \quad (2)$$

Where:  $\sigma_1, \varepsilon_1$ ——stress and strain values at the previous maximum strain point;

$\sigma_0, \varepsilon_0$ ——Stress and strain values at the latter starting strain point

Based on the mathematical model of variable elastic modulus proposed by Yoshida et al. (Ref. 21), the data points in the above three directions were fitted. The variable elastic modulus mathematical model is as follows:

$$E_{av} = E_0 - (E_0 - E_a)[1 - e^{(-\xi \varepsilon_p^a)}] \quad (3)$$

Where:  $E_{av}$ ——average elastic modulus during deformation;

$E_0$ ——initial modulus of elasticity;

$E_a, \xi$ ——Material parameters

The parameters of the variable elastic modulus equation for the three directions were fitted according to Eq. (3) and are shown in Table 3.

**Table 3 Variable elastic modulus mathematical model parameters**

Direction	$E_0/\text{GPa}$	$E_a/\text{GPa}$	$\xi$
0°	120.4	91.18	87.93
45°	113.5	88.91	84.02
90°	110.0	89.14	102.26

As shown in Fig. 4, after the comparison of the experimental data with the fitted curves, it is found that the elastic modulus in all the three directions, RD, DD, and TD, shows a significant decreasing trend with the increase of plastic strain. Taking the plastic strain 0.03 as the critical point, the elastic modulus decreases faster before the critical point and finally tends to a

constant value. With the plastic strain of 0.08, the elastic modulus decreased by 18.9% in the RD direction, 22.4% in the DD direction, and 20.0% in the TD direction.

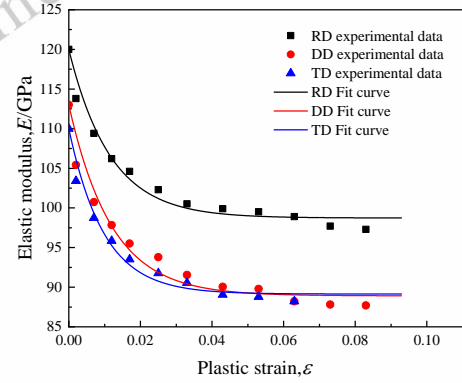


Fig.4 Variable elastic modulus fitting curve for RD, DD, TD

Figure 4 presents a high degree of overlap between the fitted curve of the mathematical model and the experimental data, indicating that the mathematical model is able to describe the changing law of elastic modulus of TC4 titanium alloy material. The three directions of TC4 titanium alloy have the same law of change, but because the initial elastic modulus of DD direction and TD direction are similar, and with the increase of plastic strain their elastic modulus has the same law of change, so the elastic modulus values of DD and TD directions are closer in the deformation process.

### 2.4 Anisotropic yield criterion

Based on the analysis of the above experimental results, it can be concluded that the TC4 titanium alloy material has obvious anisotropic characteristics, so the isotropic yield criterion is no longer applicable.

YLD2000-2D yield criterion introduces anisotropic parameters into the yield function on the basis of plane stress, which can accurately describe the yielding behavior of anisotropic materials.

The YLD2000-2D yield function expression is as follows:

$$\phi = \phi' + \phi'' = 2\bar{\sigma}^a \quad (4)$$

Where

$$\phi' = |X'_1 - X'_2|^a \quad (5)$$

$$\phi'' = |2X''_2 + X''_1|^a + |2X''_1 + X''_2|^a \quad (6)$$

where  $X'_1, X'_2, X''_1, X''_2$  are the stress principal values for  $X'$  and  $X''$ , respectively.

$$X_1 = \frac{1}{2}(X_{xx} + X_{yy} + \sqrt{(X_{xx} - X_{yy})^2 + 4X_{xy}^2}) \quad (7)$$

$$X_2 = \frac{1}{2}(X_{xx} + X_{yy} - \sqrt{(X_{xx} - X_{yy})^2 + 4X_{xy}^2}) \quad (8)$$

The components of  $X'$  and  $X''$  can be obtained by the

following two linear transformations:

$$X' = C's = C''T\sigma = L'\sigma \quad (9)$$

$$X'' = C''s = C''T\sigma = L''\sigma \quad (10)$$

$$T = \begin{bmatrix} \frac{2}{3} & -\frac{1}{3} & 0 \\ -\frac{1}{3} & \frac{2}{3} & 0 \\ 0 & 0 & 1 \end{bmatrix} \quad (11)$$

The role of the transformation matrix  $T$  is to transform the Cauchy stress  $\sigma$  into its corresponding partial stress tensor  $s$ . And the role of the matrices  $C'$  and  $C''$  is to introduce anisotropy parameters.

$$\begin{bmatrix} X'_{xx} \\ X'_{yy} \\ X'_{xy} \end{bmatrix} = \begin{bmatrix} C'_{11} & C'_{12} & 0 \\ C'_{21} & C'_{22} & 0 \\ 0 & 0 & C'_{66} \end{bmatrix} \begin{bmatrix} s_{xx} \\ s_{yy} \\ s_{xy} \end{bmatrix} \quad (12)$$

$$\begin{bmatrix} X''_{xx} \\ X''_{yy} \\ X''_{xy} \end{bmatrix} = \begin{bmatrix} C''_{11} & C''_{12} & 0 \\ C''_{21} & C''_{22} & 0 \\ 0 & 0 & C''_{66} \end{bmatrix} \begin{bmatrix} s_{xx} \\ s_{yy} \\ s_{xy} \end{bmatrix} \quad (13)$$

$$\begin{bmatrix} X'_{xx} \\ X'_{yy} \\ X'_{xy} \end{bmatrix} = \begin{bmatrix} L'_{11} & L'_{12} & 0 \\ L'_{21} & L'_{22} & 0 \\ 0 & 0 & L'_{66} \end{bmatrix} \begin{bmatrix} \sigma_{xx} \\ \sigma_{yy} \\ \sigma_{xy} \end{bmatrix} \quad (14)$$

$$\begin{bmatrix} X''_{xx} \\ X''_{yy} \\ X''_{xy} \end{bmatrix} = \begin{bmatrix} L''_{11} & L''_{12} & 0 \\ L''_{21} & L''_{22} & 0 \\ 0 & 0 & L''_{66} \end{bmatrix} \begin{bmatrix} \sigma_{xx} \\ \sigma_{yy} \\ \sigma_{xy} \end{bmatrix} \quad (15)$$

Where

$$\begin{bmatrix} L'_{11} \\ L'_{12} \\ L'_{21} \\ L'_{22} \\ L'_{66} \end{bmatrix} = \begin{bmatrix} \frac{2}{3} & 0 & 0 \\ -\frac{1}{3} & 0 & 0 \\ 0 & -\frac{1}{3} & 0 \\ 0 & \frac{2}{3} & 0 \\ 0 & 0 & 1 \end{bmatrix} \begin{bmatrix} \alpha_1 \\ \alpha_2 \\ \alpha_7 \end{bmatrix} \quad (16)$$

$$\begin{bmatrix} L''_{11} \\ L''_{12} \\ L''_{21} \\ L''_{22} \\ L''_{66} \end{bmatrix} = \frac{1}{9} \begin{bmatrix} -2 & 2 & 8 & -2 & 0 \\ 1 & -4 & -4 & 4 & 0 \\ 4 & -4 & -4 & 1 & 0 \\ -2 & 8 & 2 & -2 & 0 \\ 0 & 0 & 0 & 0 & 9 \end{bmatrix} \begin{bmatrix} \alpha_3 \\ \alpha_4 \\ \alpha_5 \\ \alpha_6 \\ \alpha_8 \end{bmatrix} \quad (17)$$

$\alpha_1 \sim \alpha_8$  are 8 anisotropic parameters, when  $\alpha_1 \sim \alpha_8$  are

equal to 1, the yield criterion is isotropic yield criterion. These eight parameters were calculated from the eight experimental data of  $\sigma_0, \sigma_{45}, \sigma_{90}, \sigma_b, r_0, r_{45}, r_{90}, r_b$  measured by uniaxial tensile experiments as well as biaxial tensile experiments in the manner of the calculation in reference to the reference 13, in which the two experimental data of  $\sigma_b, r_b$  are referenced to the reference 16, and the results of the calculation of anisotropic parameters are shown in Table 4.

Table 4 Anisotropic parameters of YLD2000-2D

YLD2000-2D parameter	Numerical value
$\alpha_1$	0.9057
$\alpha_2$	1.2511
$\alpha_3$	0.9941
$\alpha_4$	0.9906
$\alpha_5$	0.9716
$\alpha_6$	0.9674
$\alpha_7$	1.057
$\alpha_8$	1.0942
a	12

## 2.5 Numerical simulation

Numerical simulation of the five-point bending process of TC4 titanium alloy plate at room temperature is carried out using Abaqus finite element software. The numerical simulation is divided into two groups, corresponding to different bending strokes  $y = 25$  mm, 30 mm. The model dimensions and bending stroke schematic are shown in Figure 5 (unit: mm). This numerical simulation is divided into three analysis steps, the first step: the upper mold is in contact with the upper layer of the plate; the second step: bending to the specified position; the third step: the upper mold rises the plate spring back.

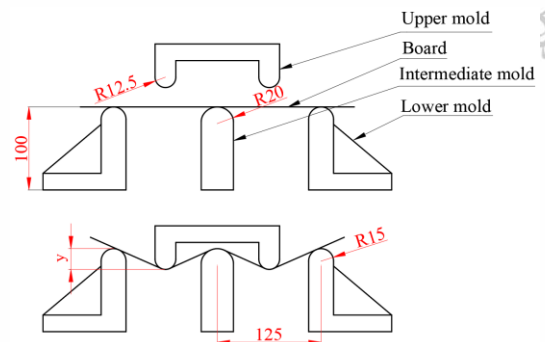


Fig.5 Schematic diagram of mold size and bending stroke

The three-dimensional model of five-point bending finite element simulation of TC4 titanium alloy plate is shown in Fig.6. The TC4 titanium alloy plate is 330 mm long, 40 mm wide and 2 mm thick, and the upper, intermediate and lower molds are set up as discrete rigid bodies, and the plate is set up as a deformable shell.



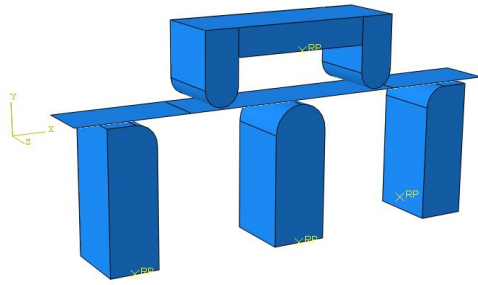


Fig.6 Finite element model

In this paper, an intrinsic model of TC4 titanium alloy was established based on the above YLD2000-2D yield criterion and variable elastic modulus mathematical model, and the model was embedded into Abaqus software through Umat subroutine interface. In order to investigate the effect of yield criterion and variable modulus of elasticity on the bending spring back prediction of TC4 plates, bending spring back simulations under three different constitutive models are carried out in this paper.

In order to accurately describe the hardening curve of TC4 titanium alloy, the Voce model is chosen in this paper to describe the variation of its flow stress. The flow stress in the rolling direction was fitted, and the fitting results are as follows:

$$\sigma_s = 1065 + 470.8 \left[ 1 - e^{-4.935 \bar{\epsilon}^p} \right] \quad (28)$$

The material parameter settings for the three constitutive models in the numerical simulations are shown in Table 6.

Table 6 Input parameters of three constitutive models

Model	YLD+Variable modulus of elasticity	YLD	Mises
Parameters			
$\alpha_1$	0.9057	0.9057	—
$\alpha_2$	1.2511	1.2511	—
$\alpha_3$	0.9941	0.9941	—
$\alpha_4$	0.9906	0.9906	—
$\alpha_5$	0.9716	0.9716	—
$\alpha_6$	0.9674	0.9674	—
$\alpha_7$	1.057	1.057	—
$\alpha_8$	1.0942	1.0942	—
$E_0/\text{GPa}$	120.4	120.4	120.4
$E_a/\text{GPa}$	91.18	—	—
$\xi$	87.93	—	—
$\nu$	0.36	0.36	0.36

Both YLD2000-2D and Mises in this paper are based on the yield criterion in the plane stress state, and the S4R four-node shell unit is used for the plate unit. In order to make the accuracy of the calculation results higher, the plate is divided into two regions to set different cell sizes, in which the deformation

of the region of the larger mesh is more fine, the deformation of the region of the smaller mesh is more coarse, the mesh is divided as shown in Figure 7.

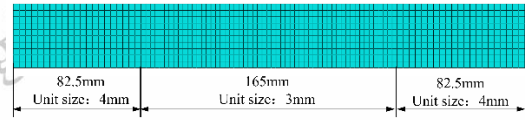
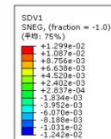


Fig.7 Element division method

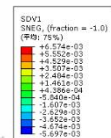
In the contact surface setup, face-to-face contact is selected as the contact type between the plate and the mold, and master-slave selection is followed, where the rigid surface is defined as the master and the deformable body surface as the slave. In addition, the contact properties are defined for the contact between the two surfaces, where the normal property is set to "hard contact", the tangential property is set to Coulomb friction, and the coefficient of friction is set to 0.2.

For the setting of boundary conditions, the upper and lower molds need to be set up with reference points, such as the RP in Fig. 8. The lower and middle molds are set up with completely fixed constraints at the reference points, and the upper mold is set up with displacement loads in the Y-axis direction at the reference points.

TC4 titanium alloy produces a very pronounced spring back phenomenon during bending due to its small modulus of elasticity. Fig.8, Fig.9 and Fig.10 show the transverse elastic strain diagrams calculated based on the "YLD+variable elastic modulus constitutive model", the YLD2000-2D anisotropic constitutive model and the Mises isotropic constitutive model for a plate with a bending stroke of 30 mm, respectively, and it can be seen that a very obvious spring back occurs after unloading of TC4 titanium alloy plates. During the bending process, the region where elastic deformation occurs is mainly concentrated in the middle region of the plate, and the elastic strain is fully recovered after spring back.

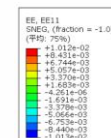


(a) Before spring back



(b) After spring back

Fig.8 Transverse elastic strain cloud based on YLD+variable modulus of elasticity for a bending stroke of 30 mm



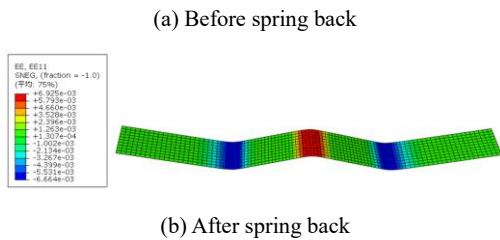


Fig.9 Transverse elastic strain cloud calculated based on YLD for a bending stroke of 30 mm

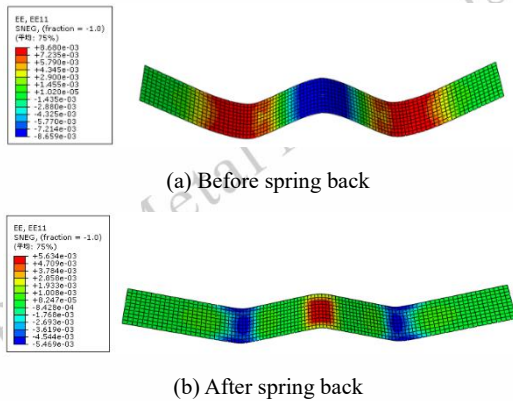
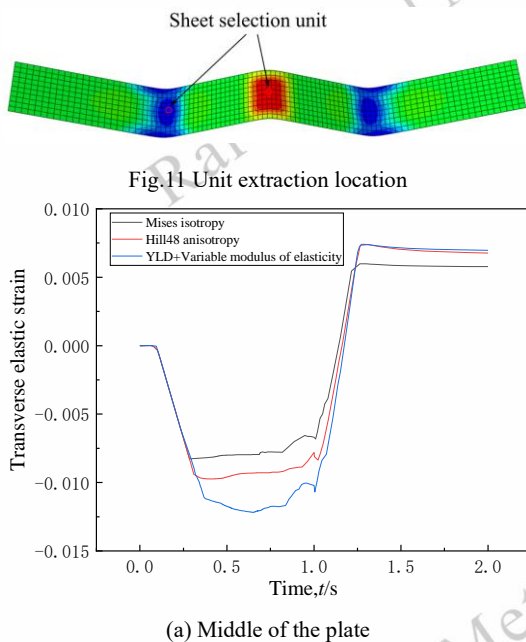
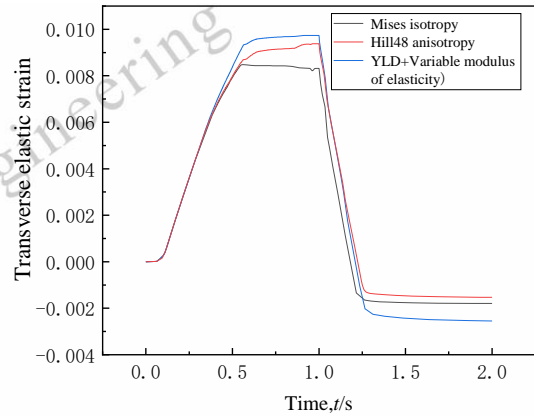


Fig.10 Transverse elastic strain cloud based on Mises calculation for a bending stroke of 30 mm

The effect of different constitutive models on the simulation results of five-point bending is visualized by deriving the variation curve of transverse elastic strain at a node with time. Fig.11 shows the cell extraction position, and Fig.12 shows the transverse elastic strain versus time curves for selected cells in the middle and left side of the plate at a bending stroke of 30 mm.



(a) Middle of the plate



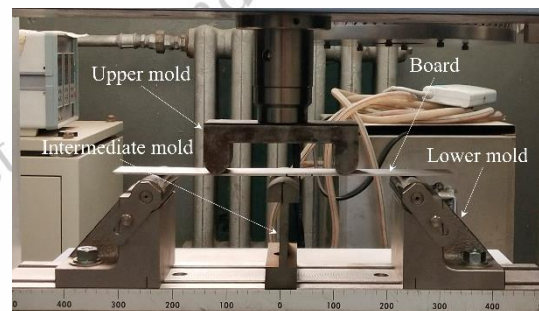
(b) Left side of plate

Fig.12 Transverse elastic strain curve of the node at  $y=30\text{mm}$

According to the transverse elastic strain curves shown in Fig.14, the "YLD+variable elastic modulus", "YLD" and Mises constitutive models have the same influence on the transverse elastic strain values of the nodes, both in the middle of the plate and on the left side of the plate. The values of transverse elastic strain calculated by numerical simulation of "YLD+variable modulus of elasticity" constitutive equation is larger than those calculated by Mises and "YLD" constitutive equations, and the value calculated by Mises isotropic constitutive model is the smallest.

## 2.6 Five-point bending test at room temperature

In order to verify the accuracy of the numerical simulation results, a five-point bending experiment of TC4 titanium alloy plate at room temperature was carried out, and this experiment was performed on an electronic universal testing machine. As shown in Fig.13, the upper mold is first affixed to the upper surface of the plate, after which the amount of under pressure is set in the operating system, the upper mold is pressed down to the specified amount of under pressure, and finally the upper mold is lifted up, and the dimensions of the mold are the same as those of the mold in the numerical simulation. The geometric parameters of TC4 titanium alloy plate used in the experiment are  $330\text{mm}\times 40\text{mm}\times 2\text{mm}$ , and the plate is processed by basic production processes such as heating, rolling, heat-straightening, heat-treating, cutting, straightening, de-phosphorizing, pickling and other basic production processes with initially rolled or forged slabs, where the heat-treating is hard annealing.



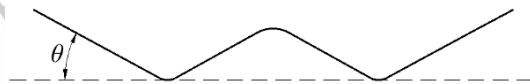
(a) Plate to mold fit diagram



(b) Plate bending diagram

Fig.13 Process flow diagram of five-point bending experiment

In this experiment, the amount of indentation was taken as 25mm and 30mm, respectively, and the schematic diagram of the experimentally measured angle  $\theta$  between the plate and the horizontal line after rebound is shown in Fig. 14.

Fig.14 Schematic diagram of the clamp angle  $\theta$ 

The final molding state of the five-point bending experiment of TC4 titanium alloy plate is shown in Fig. 15.



Fig.15 Experimental results

The experimental data for the angle  $\theta$  is shown in Table 7. In order to make the results convincing, the average of the three experiments is taken as the basis for subsequent analysis. When the bending stroke is 25mm, the angle between the plate and the horizontal line after spring back is taken as  $6.51^\circ$ ; when the bending stroke is 30mm, it is taken as  $11.12^\circ$ .

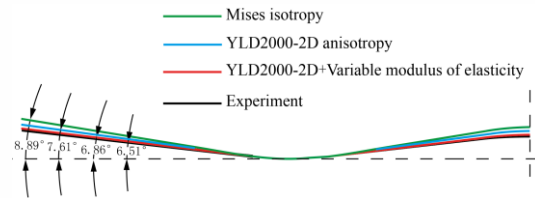
**Table 7 Angle of plate with horizontal line after spring back under different bending strokes**

Bending stroke	25mm	30mm
Experiment 1	$6.50^\circ$	$10.90^\circ$
Experiment 2	$6.17^\circ$	$11.35^\circ$
Experiment 3	$6.85^\circ$	$11.10^\circ$
Average value	$6.51^\circ$	$11.12^\circ$

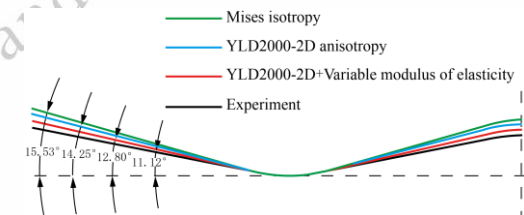
### 3 Spring back analysis

Through numerical simulation and bending experiments at room temperature, we obtained the plate spring back of TC4 titanium alloy plates under different compression bending strokes and different intrinsic models, as shown in Fig. 16 (the schematic

is the left half of the plate). The figure shows the effect of different intrinsic models on the final bending and molding results of the plates under two different bending strokes of 25mm and 30mm. The numerical simulation results based on the Mises isotropic intrinsic model have the largest gap with the experimental results for the same bending stroke. And the numerical simulation results obtained based on YLD2000-2D yield criterion and variable elastic modulus principal model are closer to the experimental results. The difference between the simulated and experimental results for the Mises isotropic principal model and the experimental results is  $2.38^\circ$  for the 25 mm bending stroke,  $1.10^\circ$  for the YLD2000-2D anisotropic constitutive model, and  $0.35^\circ$  for the YLD2000-2D yield criterion and variable elastic modulus constitutive model; at 30 mm bending stroke, the three were  $4.41^\circ$ ,  $3.13^\circ$ , and  $1.68^\circ$  from the experimental results, respectively.



(a) Bending stroke of 25 mm



(b) Bending stroke of 30 mm

Fig.16 Numerical simulation and experimental results based on different intrinsic models

As shown in Fig. 17, YLD and variable elastic modulus have higher spring back prediction accuracy compared to the other two constitutive model. The spring back prediction accuracy of YLD and variable modulus of elasticity for numerical simulation of five-point bending of TC4 titanium alloy plate under 25mm bending stroke is 11.52% and 31.18% higher than that of YLD anisotropic model and Mises isotropic constitutive model, respectively; and the spring back prediction accuracies under 30 mm bending stroke were 13.04% and 24.55% higher than those of YLD anisotropic model and Mises isotropic constitutive model, respectively. In summary, the anisotropic principal model is more suitable for the spring back prediction of TC4 titanium alloy plates, and the spring back prediction accuracy of TC4 titanium alloy plates can be significantly improved by combining with the variable elastic modulus.



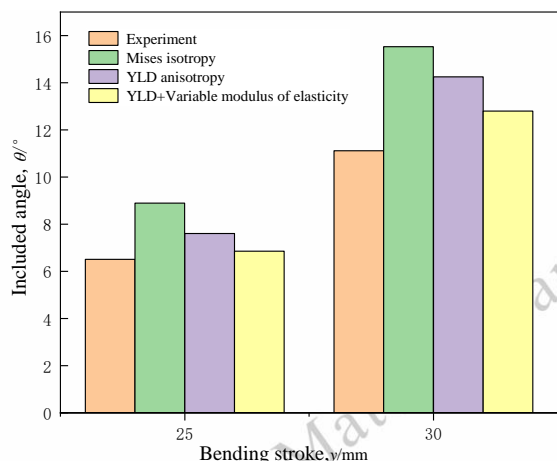


Fig. 17 Difference in spring back prediction for different constitutive models for 25mm, 30mm bending stroke

#### 4 Conclusion

This paper takes TC4 titanium alloy as the research object, based on finite element analysis, carried out a five points bending spring back prediction study of TC4 titanium alloy plate at room temperature, and reached the following conclusions:

(1) The yield strength and modulus of elasticity of TC4 titanium alloy have obvious anisotropy in RD, DD and TD directions.

(2) The modulus of elasticity of TC4 titanium alloy decreases with the increase of plastic strain and finally becomes a constant value. Based on the above law, we established a mathematical model of variable elastic modulus of TC4 titanium alloy.

(3) Based on the anisotropic yield criterion and variable modulus of elasticity, the prediction accuracy of five points bending spring back of TC4 titanium alloy plates is significantly improved, and the prediction accuracy is up to 31.18% compared with that of the isotropic principal model.

#### References

- Wang Xin, Luo Xuekun, Yu Bo et al. *Aerospace Manufacturing Technology*[J], 2022, 65(04):14-24.
- Zhou Zhongfeng, Cai Hong, Wang Yu et al. *New Technology and New Process*[J], 2022, (07):21-26.
- Li Yonghua, Zhang Wenxu, Chen Xiaolong et al. *Advances in Titanium Industry*[J], 2022, 39(01):43-48.
- J Zhao, R.X. Zhai, Z.P. Qian et al. *International Journal of Mechanical Sciences*[J], 2013, 75:45-54.
- Hao L ,Si-Rui X ,Shi-Hong Z et al. *International Journal of Mechanical Sciences*[J],2023,260
- Maati A ,Tabourot L ,Baland P et al. *Archives of Civil and Mechanical Engineering*[J],2015,15(4):836-846.
- M.U. Mert, A.Y.H. Binnaz, C.A. Sertac et al. *Journal of Materials Engineering and Performance*[J], 2022,32(10):4376-4390.
- V Esat, H Darendeliler, M.I. Gokler. *Materials & design*[J], 2002, 23(2):223-229.
- Wang Yan, Yang He, Li Heng et al. *Rare Metal Materials and Engineering*[J], 2012,41(7):1221~1225.
- M G Lee, S J Kim, H N Han. *Computational Materials Science*[J], 2009, 47(2):556-567.
- J Zhu, Y Xia, H.L. Luo et al. *International Journal of Mechanical Sciences*[J], 2014, 89:148-157.
- Ming X Y ,Ming L D ,Qi Y W et al. *Journal of Central South University*[J],2020,27(9):2578-2591
- J.W. Yoon, F Barlat, R.E. Dick et al. *International Journal of Plasticity*[J], 2004, 20(3):495-522.
- F Barlat , J.C. Brem , J.W. Yoon et al. *International Journal of Plasticity*[J], 2003, 19(9):1297-1319.
- J Naofal, H.M. Naeini, and S Mazdak. *Metals*[J], 2019, 9(9):1005.
- J.L. Chaboche. *International Journal of Plasticity*[J], 1989, 5(3):247-302.
- O.M. Badr, F Barlat, B Rolfe et al. *International Journal of Solids & Structures*[J], 2016, 80:334-347.
- Ao D ,Chu X ,Yang Y et al. *The International Journal of Advanced Manufacturing Technology*[J],2018,96(9-12):3197-3207.
- A Ghaei. *International Journal of Mechanical Sciences*[J], 2012, 65(1):38-47.
- H.Y. Yu. *Materials & Design*[J], 2009, 30(3):846-850.
- F Yoshida, T Uemori, K Fujiwara. *International Journal of Plasticity*[J], 2002, 18(5-6):633-659.
- Chen Y ,Han G ,Li S et al. *The International Journal of Advanced Manufacturing Technology*[J],2021,115(1-2):1-17.
- Liu C ,Yan D X ,Yang Y et al. *Materials Science Forum*[J],2019,4734753-760.

## 基于变弹性模量的 TC4 钛合金板材五点弯曲回弹预测

屈 聪<sup>1</sup>, 王东杰<sup>2</sup>

(1.太原科技大学机械工程学院, 山西 太原 030000)

(2.中国矿业大学机电工程学院(北京), 北京 100083)

**摘 要:** TC4 钛合金材料在弯曲过程中会产生明显的回弹, 其弹性模量对回弹有显著的影响。然而, 以往的研究没有考虑材料在塑性应变变化过程中弹性模量的变化。以 TC4 钛合金为研究对象, 通过单轴拉伸和循环加卸载实验, 确定材料的各向异性参

数以及材料弹性模量随塑性应变的变化规律。在此基础上，建立了 TC4 钛合金变弹性模量的数学模型。基于 YLD2000-2D 屈服准则和变弹性模量、YLD2000-2D 各向异性和 Mises 各向同性三种本构模型，对 TC4 钛合金板材室温五点弯曲过程进行了数值模拟。为了验证数值模拟结果，对 TC4 板材进行了室温五点弯曲试验。结果表明，各向异性本构模型和变弹性模量数学模型显著提高了 TC4 钛合金弯曲回弹的预测精度，最高预测精度提高了 31.18%。

**关键词：**钛合金；弯曲成形；变弹性模量；回弹预测

---

作者简介：屈 聪，男，1998 年生，硕士研究生，太原科技大学机械工程学院，山西太原 030000，E-mail: qc980221@163.com